



Ion irradiation damage on tin side surface of float glass

Mohammed H. Modi ^{a,*}, Gyanendra S. Lodha ^a, Manoj K. Tiwari ^a,
Sanjay K. Rai ^a, C. Mukharjee ^b, P. Magudapathy ^c,
K.G.M. Nair ^c, Rajendra V. Nandedkar ^a

^a Synchrotron Utilization Division, Centre for Advanced Technology, Indore 452 013, India

^b Laser Systems Engineering Division, Centre for Advanced Technology, Indore 452 013, India

^c Materials Science Division, Indira Gandhi Centre for Atomic Research, Kalpakkam 603 102, India

Received 28 March 2005; received in revised form 27 April 2005

Available online 15 July 2005

Abstract

Changes in the surface morphology and in-depth density variation in two surfaces of a float glass viz. the tin side and non-tin side surface, are investigated after 100 keV Ar ion irradiation. In the tin side surface, the irradiation caused a drastic change in density and surface roughness, whereas the other side (non-tin side surface) remained almost unaffected. Roughness of the tin side increases from 8 Å to 41 Å. Surface density also modified significantly with a redistribution of surface impurities. Monte Carlo simulations suggest that the displacement of tin and Fe impurities are responsible for the surface damage, which are experimentally examined by employing the total reflection X-ray fluorescence technique. Morphological and density changes are analyzed by grazing incidence X-ray reflectivity and atomic force microscopy techniques. Subsequent changes in surface morphology of float glass by ion irradiation are explained. © 2005 Elsevier B.V. All rights reserved.

PACS: 68.35.Ct; 61.10.Kw; 61.80.Jh; 79.20.Rf

Keywords: X-ray reflectivity; Ion irradiation; Float glass

1. Introduction

Stability of float glass surfaces against the corrosion has made them widely acceptable to variety

of commercial applications. It is used as a base substrate for depositing various kinds of thin film and multilayer structures. X-ray and neutron mirrors are also deposited on these substrates because of ultra low surface roughness [1]. Float glass is made by casting the soda lime material on the molten tin. This manufacturing process leads to diffusion of Sn in the surface lying in contact of molten

* Corresponding author. Tel.: +91 731 2488003; fax: +91 731 2488000.

E-mail address: modimh@cat.ernet.in (M.H. Modi).

tin bath, subsequently the two surfaces are different in chemical compositions.

Extensive studies have been carried out to understand the behavior of glass surfaces on their exposure to erosion media and high temperature environment [2,3]. Earlier, the large range of surface sensitive techniques including X-ray absorption spectroscopy, total reflection X-ray fluorescence (TXRF) spectrometry and X-ray reflectivity have been used to investigate the Sn diffusion and surface morphology [4,5]. Float glass surface that lie in contact with the molten tin during the fabrication process are found enriched with Sn and Fe impurities. It is reported the density of the tin side is higher (2.56 g/cc) in comparison to that of non-tin side (2.45 g/cc). Due to the presence of diffused Sn, a 20–50 Å thin layer on the tin side has been reported [4,6]. The Sn impurities lead to a significant change in float glass properties. In our earlier work, we have analyzed the soft X-ray optical properties of tin side surface that we found distinctly different from those of non-tin side surface [7].

Ion beam irradiation has emerged as a powerful tool to modify material properties [8]. This has been commonly used to alter the surface and interface characteristics in various thin film and multilayer samples [9,10]. Large range of semiconductor, magnetic and X-ray multilayers deposited on various substrates including float glass have been subjected to a variety of ion beam irradiation experiments [11–13]. However no work appears to have been done on the effect of ion irradiation on bare float glass substrates and its role in modifying the interfaces, intermixing etc. in deposited structures.

In the present study, we have investigated the surface morphology of float glass under the influence of low-energy Ar ions. Both tin and non-tin side surfaces of a float glass are treated by 100 keV Ar⁺ ions. Subsequent changes in surface morphology and in-depth density are analyzed by using the atomic force microscopy (AFM) and grazing incidence X-ray reflectivity (GIXR) techniques. GIXR gives electron density profile (EDP) of the materials as a function of depth, which in turn is the measure of the mass density [14]. The EDP technique is emerged as a powerful tool to analyze the surface/interface structures and is being employed to understand the chemical and

structural properties of the nanostructures near the surfaces/interfaces [15,16]. Gaythri et al. [17] have employed the technique to analyze the growth kinetics of SiO₂ film structures. Using this method, Banerjee et al. [18] have revealed the thermal swelling of SiO₂ film upon high temperature annealing. In the present study, we used the technique and revealed that ion irradiation damage occurs only on tin side surface, whereas other surface remained almost unaffected. Monte Carlo simulations are carried out to understand the atomic displacements resultant from Ar ion irradiations, which are experimentally confirmed by TXRF technique.

2. Experimental

In the present investigations, the samples used were two sides of a 2.7 mm thick float glass. During the glass solidification process the side that remained in contact with a Sn bath is called the *tin side*, and other, which remained in contact of inert environment, is called the *non-tin side*. The tin-side of float glass was identified by observing the visible fluorescence under the UV illumination. Both tin and non-tin sides of a float glass were irradiated with 100 keV Ar⁺ ions to a fluence of 3×10^{16} ions/cm² at room temperature using 150 keV ion accelerator at IGCAR, Kalpakkam, India. The beam current was limited to 0.6 μA/cm², hence the possibility of sample heating is ruled out. The samples were uniformly irradiated in 8 mm diameter, at a vacuum of 1×10^{-7} mbar. Monte Carlo simulation using SRIM 2000 code [19] shows the range of penetration of Ar⁺ ions in the float glass sample is ~1000 Å with a straggling range of ~300 Å. GIXR measurements of virgin and irradiated samples were performed using $\lambda = 1.54$ Å, Cu-K_α radiation (Philips 2KW sealed off source). An incident beam slit of 50 μm was used in combination of a knife-edge on top of the sample surface to get a beam divergence of 0.02°. NaI detector with Graphite crystal monochromator was used in diffraction arm to record the reflected beam intensity. Change in reflectivity over the six order of dynamic range was recorded. The electron density profiles from the GIXR data

were extracted using the well-known recursive formalism [20–22]. In this formalism the total thickness of the film was divided into n small slices. The electron density and roughness of each slice was varied in order to get the best fit. The non-linear least square routine based on Levenberg–Marquardt algorithm was used to refine the fit parameters.

Topographic measurements and surface roughness analysis were carried out using a multimode scanning probe microscope of NT-MDT's Solver Pro setup. AFM probe in non-contact mode and in ambient environment was used. Silicon cantilever at resonant frequency ~ 180 kHz and spring constant 5.5 N/m were employed.

Total reflection X-ray fluorescence measurements were performed on an in-house developed TXRF spectrometer [23]. The fluorescence data were taken using a Peltier cooled solid state detector [Eurisys Mesures EPXR 10-300], having an energy resolution of 250 eV at 5.9 keV. A well-collimated primary beam, from a line focus Cu X-ray tube, was used as an excitation source.

3. Results and discussions

3.1. Virgin samples

Fig. 1 show the GIXR spectra of the tin and non-tin sides of a float glass. For clarity, the GIXR curve of tin side is shifted vertically up. The inset shows the close view of critical angle region, which clearly indicates higher density of the tin side in comparison to that of the non-tin side.¹ The mass density comes out to be 2.62 g/cc and 2.25 g/cc for the tin side and non-tin side respectively. The electron density profiles of both sides, for the virgin sample, are plotted in Fig. 2. Due to the presence of a low-density layer, the density rises slowly near the surface that is marked as region 'A'. Thickness of low density or contamination layer is found to be in the 7–8 Å range. The electron density reaches to the substrate density, marked by region 'C', via

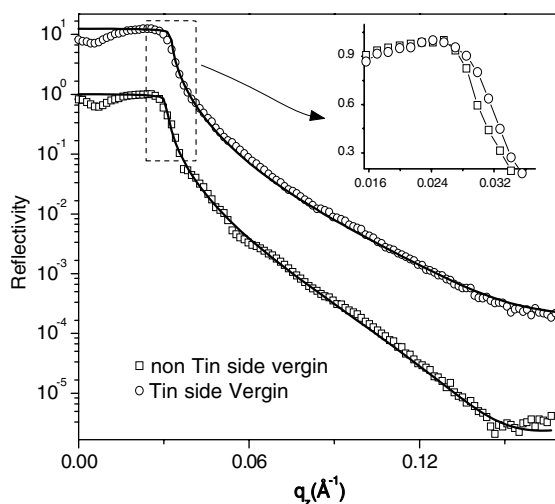


Fig. 1. Experimental and fitted reflectivity curve of the tin side and non-tin side of a float glass as a function of wave vector q_z (\AA^{-1}) for virgin samples. In inset the critical angle region is shown, where the curve corresponding to tin side shows higher value of critical angle due to higher surface density.

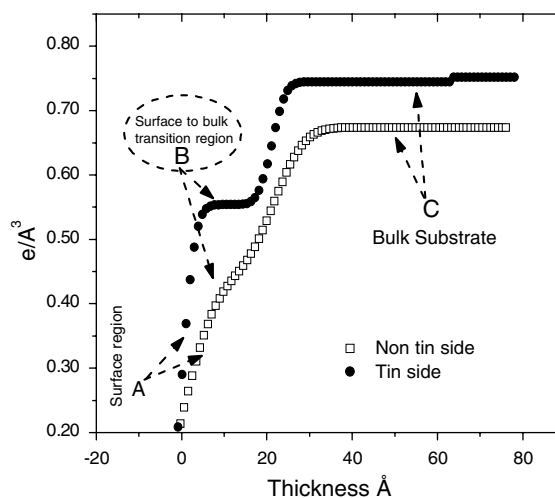


Fig. 2. EDP for the tin side and non-tin side of virgin samples are shown. Regions marked by labels 'A', 'B' and 'C' are corresponding to surface, transition and substrate density regions as explained in the text.

the transition region 'B'. Signature of transition layer is distinctly visible in EDP profile of the tin side case. This transition layer thickness is 21 Å and electron density $0.55 \text{ e}/\text{\AA}^3$, as calculated from EDP. The density of this layer is 73% of substrate

¹ Critical angle for total external reflection θ_c is directly proportional to square root of electron density of the material ρ_e .

density (substrate density of the tin side is $0.75 \text{ e}/\text{\AA}^3$). In case of the non-tin side, a small hump in EDP profile at 12 \AA depth is corresponding to the signature of transition layer for this side. Transition layer on the non-tin side has the density 66% of the bulk value.

The origin of transition layer on the tin side is understandable due to the presence of a diffused Sn and Fe impurities [4]. Whereas, a small hump in density profile of the non-tin side sample may be arising from the solidification process. During solidification, the non-tin side of a glass quenched more rapidly than the tin side, because the tin side remains in contact of hot liquid tin. Huppaufl and Lengeler [4] have also shown the presence of a transition layer on both the sides of a float glass and termed it as surface layer. Their thickness and density values for this transition layer on either side of the float glass are same i.e. thicknesses 54 \AA and density 89% of bulk. This is physically unrealistic as two respective surfaces of a float glass passes through different solidification environment. In fact, our results clearly indicate the difference between transition layers formed on two respective surfaces. The presence of a contamination or low density layer just near the surface, have been reported by various authors in different materials studied by GIXR technique, and it is shown that this layer does not have any physical importance [17,24].

3.2. Ion irradiated samples

In Fig. 3 the effect of ion irradiation on tin side is shown. The inset of the figure shows the EDP profiles of virgin and irradiated samples. From the EDP profile it is evident that there is a major change in tin side after 100 keV Ar^+ ion irradiation. The electron density gradually increases near the surface (open circles), whereas in case of virgin sample (open triangle) the electron density varies rapidly. Such changes correspond to either porosity or higher surface roughness that we have confirmed by AFM technique and discussed in succeeding section. In the inset of Fig. 3, the surface region is marked as 'R1' and bulk region where electron density reaches to substrate density is marked as 'R2'. The 'transition layer' of the vir-

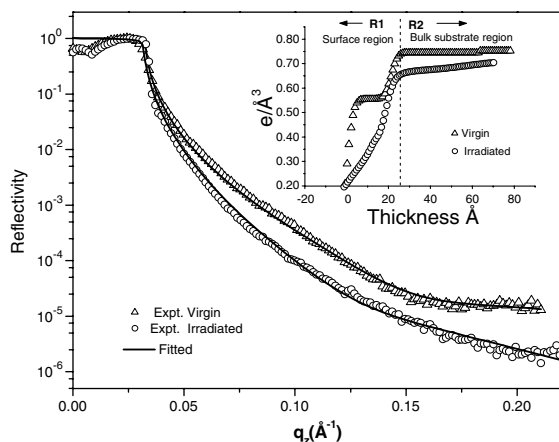


Fig. 3. Measured and fitted reflectivity curve of the tin side of float glass, before and after ion beam irradiation. The scattered points are corresponding to measured data, whereas continuous line represents the best fit. In inset the EDP obtained from the fit is shown for both the cases. The effect of irradiation is described in the text.

gin sample vanishes after irradiation (see EDPs in region R1), which indicates a major change in atomic distribution near the surface of the tin side. In region R2, the electron density of the irradiated sample (open circles) gradually reaches the substrate density but does not attain a constant value as we found in virgin sample (open triangle). It gradually increases from $0.65 \text{ e}/\text{\AA}^3$ to $0.70 \text{ e}/\text{\AA}^3$ in region R2 of the irradiated sample, whereas it shows a constant behavior in virgin sample.

In Fig. 4, we show the GIXR spectra of virgin and ion irradiated samples of non-tin side float glass. The inset shows the change in EDP profile compared to the virgin sample. The EDP profile shows a small change in surface and bulk density after the irradiation. The profile near the surface is almost similar suggesting both surface roughness and composition are not changed significantly. The substrate density is marginally changed by 2.9%, which can be due to the embedded Ar.

AFM measurements of tin and non-tin sides, after ion irradiations, are shown in Fig. 5. After irradiation, rms roughness estimated from AFM images is 41 \AA and 13 \AA for tin side and non-tin side, respectively. Before irradiation the corresponding rms roughness values are 8.1 \AA and

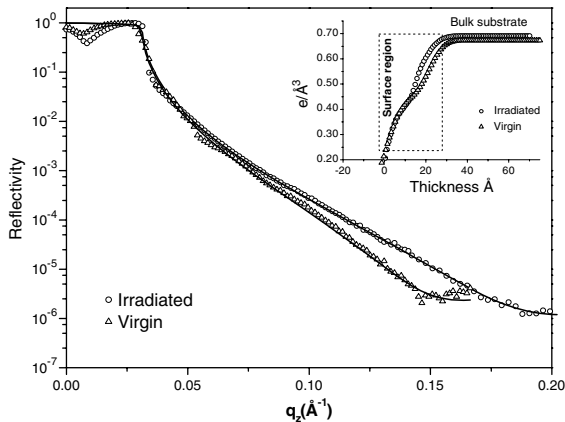
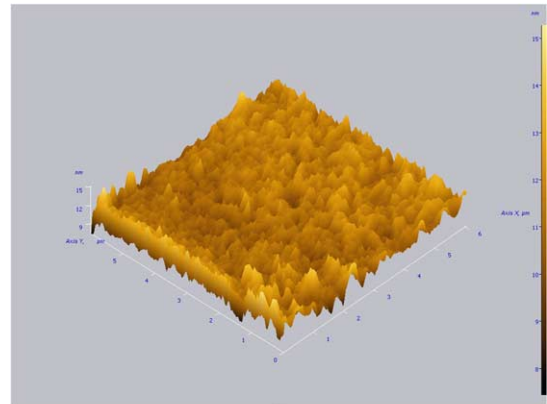


Fig. 4. Measured and fitted reflectivity curve of the non-tin side of float glass, before and after ion beam irradiation. The scattered points are corresponding to measured data, whereas continuous line represents the best fit. In inset the EDP obtained from the fit is shown for both the cases. The effect of irradiation is described in the text.

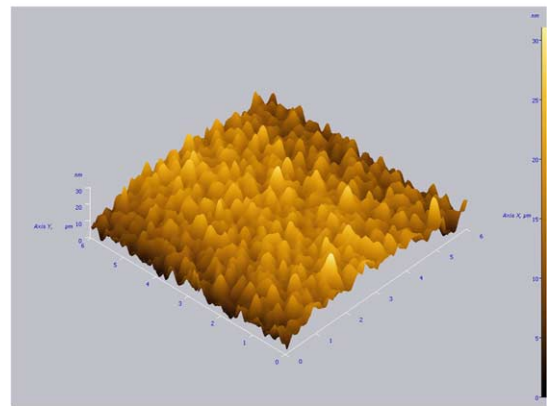
4.8 Å. AFM results confirm the drastic change in surface of the tin side as revealed by EDP. In EDP, we have observed that the electron density gradually increases in surface region R1 (Fig. 3 inset), which could be due to either porosity or roughness, but with AFM images it is confirmed that the roughness is increased. AFM results show a ~ 2.5 times change in surface roughness of the non-tin side which is much smaller than the change in roughness of the tin side. Except a marginal change in roughness, the non-tin side is more stable than the tin side of a float glass against 100 keV Ar ion irradiations.

In order to understand the effect of ion irradiation on the tin and non-tin side, we have carried out Monte Carlo simulation study using the SRIM 2000 code. For the non-tin side, we used the composition of soda lime glass provided in the code with a density of 2.45 g/cm³ (Si 25 at.%; O 60 at.%; Na 11 at.%; Ca 3 at.%; Mg and Al 1 at.% each). For the tin side, we have considered the density of 2.56 g/cm³ by adding the impurities of Sn – 9.2 at.%, and Fe – 6.7 at.% with a uniform distribution.² The results of Monte Carlo simulation using 5000 incident Ar⁺ ions of 100 keV are

² In [5], the tin diffusion over several microns is reported.



a



b

Fig. 5. AFM images obtained for (a) non-tin side and (b) tin side surfaces after the 100 keV Ar ion irradiations. The tin side surface of float glass is roughened significantly than the non-tin side surface after ion irradiation.

plotted in Fig. 6. As SiO₂ is a major constituent of soda lime glass, in Fig. 6(a) we show the recoil distribution of Si in the tin and non-tin sides. For silicon, the displacement energy of 15 eV is considered and results show that the silicon recoil distribution is different in two respective surfaces. The silicon recoil distribution changes gradually on the tin side whereas it varies rapidly on the non-tin side.

For the tin side, in Fig. 6(b) recoil distributions of Sn and Fe impurities are plotted assuming the displacement energy of 25 eV. The results suggest that Si, Sn and Fe are segregating in the bulk, creating the voids near the surface, which are responsible for increasing surface roughness. As Sn and

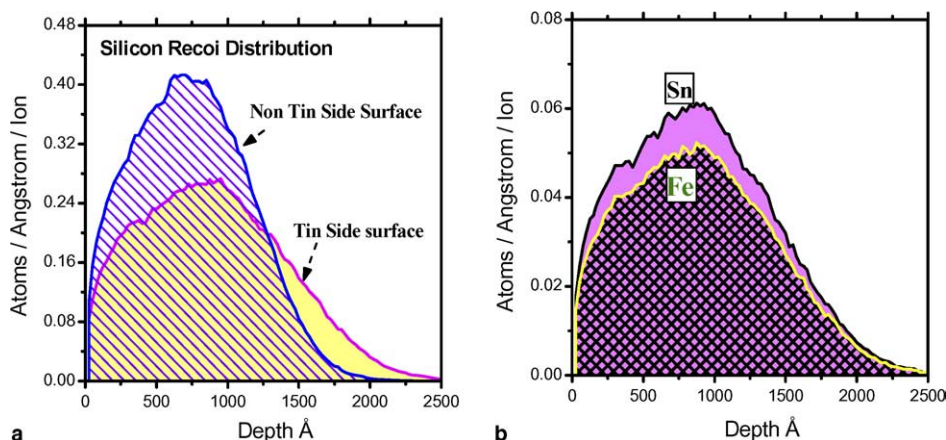


Fig. 6. Distribution of displaced (a) Si (b) Fe and Sn atoms under the influence of 100 keV Ar irradiation in soda lime glass as calculated using SRIM 2000 code.

Fe are bigger and heavier in comparison to Si, so their displacement from the surface will result in more increase in surface roughness. Their displacement will further affect the surface density more prominently in comparison to displacement of silicon atoms. Hence the tin side is modified significantly by ion irradiation in comparison to the non-tin side. The values of sputtering yield, as calculated by SRIM 2000 code for both the surfaces is in the range of 2.1–2.2 atoms/ion, which suggest that the sputtering is not modifying the surface. Another possibility of blister formation, which can also increase the roughness, is ruled out as the dose is below the critical dose required for blister formation [25].

To verify the theoretical calculations and possible mechanism of irradiation damage in tin side of float glass, further experiments using the TXRF method were carried out by observing the fluorescence intensity of float glass constituents near the surface. The fluorescence spectra are recorded using the Cu-K α monochromatic radiation as an excitation source at an incidence angle of 0.229° (close to critical angle) where the penetration depth is \sim 600 Å so that only subsurface atoms give X-ray fluorescence. In Fig. 7, results of TXRF measurements of the non-tin side of virgin and irradiated samples are plotted. Due to change in excitation efficiency of X-ray lines of various elements, a strong peak corresponding to Ca-K α

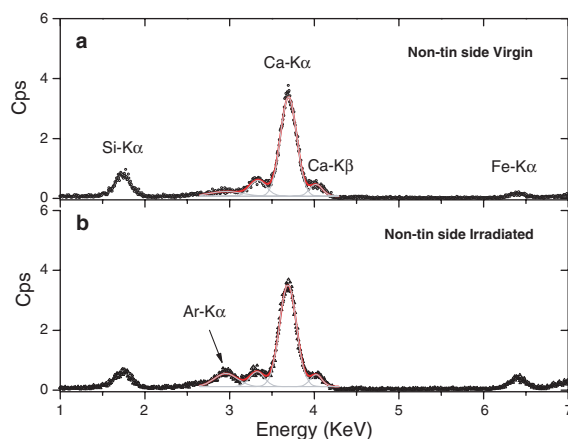


Fig. 7. TXRF spectrum of the non-tin side (a) before irradiation and (b) after irradiation. Spectrum is recorded with Cu-K α monochromatic radiations as an excitation source at an incidence angle of 0.229°. From (b) it is evident that the Ar is embedded inside the surface.

(3.69 keV) and the small peaks of Si-K α (1.74 keV) and Fe-K α (6.40 keV) are detected. After irradiation, the intensity of Si peak is reduced (\sim 40%), which corresponds to change in Si distribution as predicted by the Monte Carlo simulations. The Ar embeds in float glass matrix after the irradiation, which compensates the change in Si concentration, and the resultant density profile of the non-tin side does not change

significantly. A minor increase in intensity of Fe peak could not be understood.

Measured TXRF spectra for tin side surface, for virgin and irradiated sample, are plotted in Fig. 8. In this case, the fluorescence peaks of Si, Ca and Fe, in addition to the fluorescence peak of Sn-L α (3.44 keV) are detected. Due to limited detector resolution of 250 eV, peaks corresponding to Ca-K α and Sn-L α could not be well separated and spectrum unfolding is done using the non-linear least square fitting method. Furthermore, the intensity of silicon in tin side does not change after irradiation and that means the concentration of silicon is not affected. It could be understood as the presence of a diffused Sn and Fe impurities, which forms a layer near the surface, interacts strongly with incident ion beam due to the large atomic volume and contribute in added atomic displacement by repeated collisions with other atoms. Interestingly, TXRF spectrum also confirms the change in Sn concentration, as the intensity of Sn-L α is reduced significantly (30%) after the irradiation (Fig. 8(b)) and the peak corresponding to embedded Ar is observed in subsurface region. The intensity of Fe-K α line is reduced (by 20%) due to its displacement from sur-

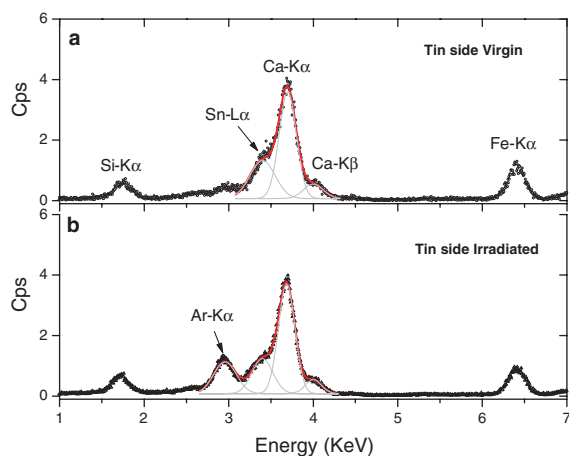


Fig. 8. TXRF spectrum of tin side (a) before irradiation and (b) after irradiation. Fluorescence spectrum is recorded at an incidence angle of 0.229° (Cu-K α monochromatic excitations) so that only the surface elements contribute in fluorescence signal. Details are given in the text.

face to the bulk as suggested by Monte Carlo simulations. Our EDP profile for tin side surface (Fig. 3) provides the experimental proof to the fact that the more atoms are systematically displaced from the surface into the bulk. Because of this displacement, the density is reduced near the surface and it increases gradually inside the bulk substrate. For the non-tin side, both Monte Carlo simulation as well as the experimental EDP profile, AFM image and TXRF measurements revealed that the surface is more stable against the ion bombardment.

It is common that the float glasses are used for depositing various kinds of thin film/multilayer mirrors and those are also subjected to ion irradiation experiments [11–13,26]. Ghose et al. [11] have irradiated Pt/C multilayer deposited on float glass by 2 MeV Au ions and reported the change in interface roughnesses. However, they have not mentioned about which side of float glass used for depositing the multilayer structures. Similarly, Paul et al. [13] have also reported the change in interface width of Fe/Cr multilayer deposited on float glass under the influence of 200 MeV Ag ions. Our study clearly reveals the fact that the two surfaces of float glass are distinctly different and more interestingly their susceptibility to ion damage experiments are also different. The roughness and density of tin side surface modifies drastically after the irradiation so in the case where float glass is used as a base substrate (in multilayer studies), the role of float glass itself in interface mixing/broadening cannot be ruled out. Further experiments are required to analyze the effect of float glass surfaces in different kind of ion irradiation experiments.

4. Conclusions

Both tin and non-tin side surfaces of a float glass are irradiated with 100 keV Ar ion with a fluence of 3×10^{16} ions/cm 2 . These surfaces are experimentally examined by GIXR, AFM and TXRF techniques to analyze the surface morphology and in-depth density distribution. The electron density profiles obtained for tin and non-tin sides explained the basic differences between two

surfaces. In tin side, there is a clear mark of formation of an additional layer near the surface due to the presence of a diffused Sn and Fe impurities. When this side is subjected to ion irradiation, the impurity enriched layer vanishes (EDP profile Fig. 3). Sn and Fe impurities segregate inside the bulk and resultant displacement cause the damage near the surface. Since, the composition of non-tin side surface is uniform, so after irradiation the Ar ions are embedded in the bulk matrix, which results in a marginal change in density (EDP profile Fig. 4). After irradiation, AFM images show a drastic change in roughness of tin side whereas it does not change much for non-tin side. TXRF results provide a distinct proof of changes in Sn concentration near the surface, which causes for change in the surface density.

References

- [1] Z. Yin, L. Berman, S. Dierker, E. Defresne, D.P. Siddons, in: L.E. Berman, J. Arthur (Eds.), *Optics for high brightness synchrotron radiation beamlines II*, Proc. SPIE, Vol. 2856, 1996, p. 307.
- [2] A. Gorokhovskiy, K. Matzov, J.I. Escalante-Garcia, *J. Non Cryst. Solids* 291 (2001) 43.
- [3] R.M. Richardson, R.M. Dalgliesh, T. Brennan, M.R. Lovell, A.C. Barnes, *J. Non-Cryst. Solids* 292 (2001) 93.
- [4] M. Huppaufl, B. Lengeler, *J. Appl. Phys.* 75 (1994) 785.
- [5] K.F.E. Williams, C.E. Johnson, O. Nikolov, M.F. Thomas, J.A. Johnson, J. Greengrass, *J. Non Cryst. Solids* 242 (1998) 183.
- [6] P.J. LaPuma, R.L. Snyder, S. Zdziszynski, R. Bruckner, *Adv. X-ray Anal.* 38 (1995) 705.
- [7] M.H. Modi, G.S. Lodha, K.J.S. Sawhney, R.V. Nandedkar, *Appl. Optics* 42 (2003) 6939.
- [8] M. Kopcewicz, A. Dunlop, *J. Appl. Phys.* 90 (2001) 74.
- [9] W. Bolse, B. Schattat, *Nucl. Instr. and Meth. B* 190 (2002) 173.
- [10] S. Amirthapandian, B.K. Panigrahi, A.K. Srivastav, S. Dhara, A. Gupta, V.S. Sastry, R.V. Nandedkar, K.G.M. Nair, A. Narayanasamy, *J. Appl. Phys.* 95 (2004) 5295.
- [11] S.K. Ghose, D.K. Goswami, B. Rout, B.N. Dev, *Appl. Phys. Lett.* 79 (2001) 467.
- [12] N. Bajwa, A. Ingale, D.K. Avasthi, Ravi Kumar, K. Dharamvir, V.K. Jindal, *Nucl. Instr. and Meth. B* 212 (2003) 233.
- [13] A. Paul, A. Gupta, S.M. Chaudhari, D.M. Phase, *Vacuum* 60 (2001) 401.
- [14] J.K. Basu, M.K. Sanyal, *Phys. Rep.* 363 (2002) 1.
- [15] S. Pal, M.K. Sanyal, S. Hazra, S. Kundu, F. Schreiber, J. Pflaum, E. Barrena, H. Dosch, *J. Appl. Phys.* 95 (2004) 1430.
- [16] S. Banerjee, A. Gibaud, D. Chateigner, S. Ferrari, M. Fanciulli, *J. Appl. Phys.* 95 (2002) 540.
- [17] N. Gayathri, S. Banerjee, *Appl. Phys. Lett.* 84 (2004) 5192.
- [18] S. Banerjee, S. Chakraborty, P.T. Lai, *Appl. Phys. Lett.* 80 (2002) 3075.
- [19] J.F. Ziegler, SRIM 2000, IBM NY.
- [20] S. Banerjee, S. Ferrari, D. Chateigner, A. Gibaud, *Thin Solid Films* 450 (2004) 23.
- [21] S. Banerjee, S. Ferrari, R. Piagge, S. Spandoni, *Appl. Phys. Lett.* 84 (2004) 3798.
- [22] L.G. Parratt, *Phys. Rev.* 95 (1954) 359.
- [23] M.K. Tiwari, B. Gowrishankar, V.K. Raghuvanshi, R.V. Nandedkar, K.J.S. Sawhney, *Bull. Mater. Sci.* 25 (2002) 435.
- [24] J.M. Grimal, P. Chartier, P. Lehuédé, *J. Non-Cryst. Solids* 196 (1996) 128.
- [25] R.V. Nandedkar, Private communication.
- [26] T. Blon, G. Ben Assayag, D. Chassaing, D. Hrabovsky, J.F. Bobo, J.C. Ousset, E. Snoeck, *J. Appl. Phys.* 95 (2004) 8030.